

This is the accepted manuscript made available via CHORUS. The article has been published as:

Photoproduction of the $f_{\{2\}}^{\{'\}}(1525)$, $a_{\{2\}}(1320)$, and $K_{\{2\}}^{\{*\}}(1430)$

Ju-Jun Xie, E. Oset, and Li-Sheng Geng

Phys. Rev. C **93**, 025202 — Published 8 February 2016

DOI: [10.1103/PhysRevC.93.025202](https://doi.org/10.1103/PhysRevC.93.025202)

Photoproduction of the $f'_2(1525)$, $a_2(1320)$ and $K_2^*(1430)$

Ju-Jun Xie,^{1,2,3} E. Oset,^{1,4} and Li-Sheng Geng^{5,3,*}

¹*Institute of Modern Physics, Chinese Academy of Sciences, Lanzhou 730000, China*

²*Research Center for Hadron and CSR Physics, Institute of Modern Physics of CAS and Lanzhou University, Lanzhou 730000, China*

³*State Key Laboratory of Theoretical Physics, Institute of Theoretical Physics, Chinese Academy of Sciences, Beijing 100190, China*

⁴*Departamento de Física Teórica and IFIC, Centro Mixto Universidad de Valencia-CSIC Institutos de Investigación de Paterna, Aptdo. 22085, 46071 Valencia, Spain*

⁵*School of Physics and Nuclear Energy Engineering and International Research Center for Nuclei and Particles in the Cosmos, Beihang University, Beijing 100191, China*

(Dated: January 5, 2016)

Assuming that the $f'_2(1525)$, $a_2(1320)$ and $K_2^*(1430)$ resonances are dynamically generated states from the vector meson-vector meson interactions in S -wave with spin $S = 2$, we study the $\gamma p \rightarrow f'_2(1525)p$, $\gamma p \rightarrow a_2^0(1320)p$ and $\gamma p \rightarrow K_2^*(1430)\Lambda(\Sigma)$ reactions. These reactions proceed in the following way: the incoming photon first mutates into a ρ^0 , ω , or ϕ meson via vector meson dominance, which then interacts with the ρ^0 , ω or K^* emitted by the incoming proton to form the tensor mesons $f'_2(1525)$, $a_2(1320)$ and $K_2^*(1430)$. The picture is simple and has no free parameters, as all the parameters of the mechanism have been fixed in previous studies. We predict the differential and total cross sections of these reactions. The results can be tested in future experiments and therefore offer new clues on the nature of these tensor states.

PACS numbers: 13.60.Le, 13.75.Lb, 14.40.Cs

I. INTRODUCTION

Recent observations of the new baryonic P_c states [1] and the mesonic XYZ states [2–5] by various collaborations have challenged the conventional wisdom that mesons are made of quark-antiquark pairs and baryons are composed of three quarks in the naive quark model. These findings have attracted a lot of attention from the theory side. Various explanations of these states have been proposed, such as molecules, multiquark compact objects, kinematic effects, or mixtures of components of different nature. Up to now none of them has been accepted unanimously. This is not surprising, given limited experimental constraints and the fact that the various components of a hadron are not observables themselves. Furthermore, it is quite likely that a specific reaction or decay process can only review part of the nature of the hadrons under investigation. Clearly, the only way to understand the nature of a hadron is to examine it from all possible ways, both experimentally and theoretically.

Nevertheless, it seems clear that Nature is richer than it is preferred to be. In this respect, it is not surprising to find out that many low-lying states, even those long believed to be conventional $q\bar{q}$ (or qqq) states, may have large components of other nature. Indeed, it has been shown that many of the low-lying mesonic states can be understood not only as $q\bar{q}$ states but also as meson-meson molecules, dynamically generated in the so-called unitary approaches. One of such examples are the tensor states: $f_2(1270)$, $f'_2(1525)$, $a_2(1320)$, and $K_2^*(1430)$. They are found dynamically generated from the vector meson-vector meson interactions [6–9],¹ obtained in the coupled-channel Bethe-Salpeter equations by unitarizing the tree-level hidden gauge diagrams [12–15]. **When stating that these states are molecular states one is implying that these are the main components of an admittedly complex structure. As discussed below, there is plenty of phenomenological support for it for the case of the $f_2(1270)$, $f'_2(1525)$ and $K_2^*(1430)$. The case of the $a_2(1320)$ might need more important non molecular components, as we shall discuss.**

The molecular nature of these tensor states has been extensively tested in a large number of processes, for instance, the two-photon decay of the $f_2(1270)$ [16]; the two-photon and one photon-one vector decays of the $f_2(1270)$, $f'_2(1525)$ and $K_2^*(1430)$ [17]; the $J/\psi \rightarrow \phi(\omega)f_2(1270)$, $f'_2(1525)$ and $J/\psi \rightarrow K^{*0}(892)\bar{K}_2^{*0}(1430)$ decays [18]; the radiative decay of J/ψ into $f_2(1270)$ and $f'_2(1525)$ [19]; the $\psi(2S)$ decays into $\omega(\phi)f_2(1270)$, $\omega(\phi)f'_2(1525)$, $K^{*0}(892)\bar{K}_2^{*0}(1430)$ and

*Electronic address: lisheng.geng@buaa.edu.cn

¹ It should be noted that vector meson-vector meson interactions and the resulting molecular states have been recently discussed in potential models [10] and quark models [11] as well.

the radiative decays of $\Upsilon(1S)$, $\Upsilon(2S)$, $\psi(2S)$ into $\gamma f_2(1270)$, $\gamma f'_2(1525)$, $\gamma f_0(1370)$, and $\gamma f_0(1710)$ [20, 21]; the ratio of the decay widths of $\bar{B}_s^0 \rightarrow J/\psi f_2(1270)$ to $\bar{B}_s^0 \rightarrow J/\psi f'_2(1525)$ [22]. The agreement with experimental data turns out to be quite good in general, providing support to the underlying assumption that these states contain large meson-meson components. The decays of the $K_2^*(1430)$ into $K\gamma$ and of one a_2 state found in Ref. [7] into $\pi\gamma$ were also studied in Ref. [9] and found to be in qualitative agreement with data if the a_2 state is associated to the $a_2(1320)$, as we shall do here.

In a recent work [23], taking the molecular picture for the $f_2(1270)$ resonance, the $\gamma p \rightarrow p f_2(1270)$ reaction has been studied. It was found that the theoretical results of the differential cross sections are in agreement with the experimental data of Ref. [24], providing first support for the molecular picture of the $f_2(1270)$ state in a baryonic reaction. In this work, we extend the formalism proposed in Ref. [23] to study the $\gamma p \rightarrow f'_2(1525)p$, $\gamma p \rightarrow a_2^0(1320)p$, and $\gamma p \rightarrow K_2^*(1430)\Lambda(\Sigma)$ reactions. One should stress again that as the only way to unravel the nature of a hadron is via different reactions and decay processes, we deem such studies very timely and important.

We should note that the picture offered here for these tensor mesons is relatively novel and most of the previous work has made different assumptions for their nature. Reviews on the properties and nature of mesons can be found in Refs. [25, 26]. For the concrete case of tensor mesons a good review is made in Ref. [27] where methods used by different groups are discussed, including effective Lagrangian approaches based on vector- and tensor-meson dominance, quark models with possible meson-glueball mixing, current-algebra approach, lattice QCD, QCD sum rules, the 3P_0 model, chiral perturbation theory, Regge model, dispersion-relation technique, and others. More related to our work here is the one of Ref. [28] where the tensor mesons are associated to meson multiplets and their couplings to pseudoscalar mesons are interpreted in the framework of chiral resonance Lagrangians [29, 30], but no reference to the internal structure of the states ($q\bar{q}$, multi-quark states, meson-meson bound states, glueballs, etc) is made. Using the same mixing angle between a singlet and an octet of $SU(3)$ assumed in Ref. [28], it is found in Ref. [27] that the $f'_2(1525)$ decays more strongly in $K\bar{K}$ than in $\pi\pi$, as found in experiments. This property is also respected in the approach of Ref. [7] (see table I of Ref. [31]) since this resonance is mostly made of $K^*\bar{K}^*$, which decays both in $K\bar{K}$ and $\pi\pi$, by means of the decays of a K^* into $K\pi$, having a virtual π or a virtual K connected with the other \bar{K}^* . The case with the virtual π leads to $K\bar{K}$ and is more favorable, because of the light mass of the π , than when the K is virtual and one has then two π in the final state. **Yet, there are also differences between the approach followed here and the one in [28]. In this latter work the states are assumed to be composed of octets and singlets of $SU(3)$ and follow a $SU(3)$ breaking pattern linear in the quark masses. In the molecular case the two octets of the vector mesons give rise to a singlet, two octets, the 10, $\bar{10}$, and 27 $SU(3)$ representations with attraction in some of these channels. The $SU(3)$ breaking pattern is also different, based on the local hidden gauge approach for the Lagrangians and mostly on the use of the unitarization procedure in coupled channels, with physical masses of the particles which ensure good analytical properties and proper threshold behavior if the masses of the states appear close to two particle thresholds. A detailed study of the $SU(3)$ structure of such states for the case of baryons is done in [32] and [33].**

The explicit interaction of vector mesons pairs has also been addressed more recently in Refs. [34, 35] from the formal point of view and focusing on its use in dispersions relations of unitary schemes in coupled channels. In Ref. [35], the generic structure of partial-wave projected t - and u -channel exchange diagrams was analyzed. A general and explicit form for a dispersion-integral representation for their contributions to partial-wave reaction amplitudes was established. Closer to the work of Ref. [7] and also making predictions for states dynamically generated is the work of Ref. [36]. In this work an $SU(6)$ spin-flavor symmetry is invoked, but imposing a breaking of this symmetry that generates the Weinberg Tomozawa interaction. The same states as in Ref. [7] are obtained. The results also share the difficulties in getting the $a_2(1320)$ resonance, which in Ref. [7] appears around 1567 MeV, with the standard subtraction constants, while in Ref. [36] is obtained using an unusual large cutoff of $3 \sim 4$ GeV. We shall take this into account by admitting larger uncertainties for this resonance in our final results.

The present article is organized as follows. In Sec. II, we introduce the formalism and the main ingredients of the model. In Sec. III, we present our main results, and a short summary and conclusions are given in Sec. IV.

II. FORMALISM AND INGREDIENTS

A. Feynman amplitudes

From the perspective that the $f'_2(1525)$, $a_2(1320)$ and $K_2^*(1430)$ resonances are dynamically generated from the vector-vector (VV) interactions, the $f'_2(1525)$, $a_2(1320)$ and $K_2^*(1430)$ photoproductions proceed via the creation of two vector mesons by the γp initial state in a primary step and the following interaction (rescattering) of the two vector mesons, thus dynamically generating the resonance. The corresponding Feynman diagrams are shown in Fig. 1 for the $\gamma p \rightarrow f'_2(1525)p$ and $\gamma p \rightarrow a_2^0(1320)p$ reactions and Fig. 2 for the $\gamma p \rightarrow K_2^*(1430)\Lambda(\Sigma)$ reaction.

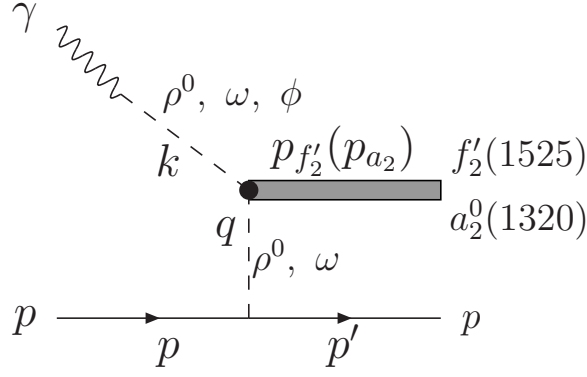


FIG. 1: Diagrammatic representation of the $f'_2(1525)$ and $a_2^0(1320)$ photoproduction, where k , p , p' , q , $p_{f'_2}$, p_{a_2} are the four-momentum of the involved particles and $q = p' - p$.

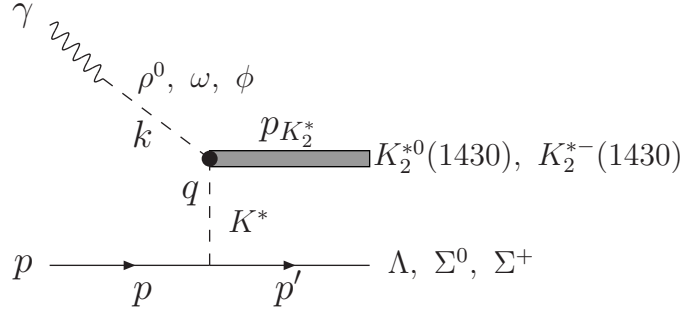


FIG. 2: Diagrammatic representation of the $\gamma p \rightarrow K_2^*(1430)\Lambda(\Sigma)$ reaction.

As can be seen from Figs. 1 and 2, the photon first gets converted into one vector meson, a characteristic of the local hidden gauge formalism, which then interacts with the other vector emitted by the proton. To evaluate the Feynman amplitudes, we need the coupling of the tensor meson to the respective vector mesons, g_T^{VV} , the γ - V coupling, and the VNN coupling. In the unitary approach, the amplitude close to a pole that represents a resonance can be written in the following way

$$t_{\text{pole}} \simeq \frac{(g_T^{VV})^2 P_{\text{initial}}^{(2)} P_{\text{final}}^{(2)}}{s - s_R}, \quad (1)$$

$$P_{\text{initial}}^{(2)} = \frac{1}{2}(\epsilon_i^{(1)} \epsilon_j^{(2)} + \epsilon_j^{(1)} \epsilon_i^{(2)}) - \frac{1}{3} \epsilon_l^{(1)} \epsilon_l^{(2)} \delta_{ij}, \quad (2)$$

$$P_{\text{final}}^{(2)} = \frac{1}{2}(\epsilon_i^{(3)} \epsilon_j^{(4)} + \epsilon_j^{(3)} \epsilon_i^{(4)}) - \frac{1}{3} \epsilon_m^{(3)} \epsilon_m^{(4)} \delta_{ij}, \quad (3)$$

where s_R is the pole position and g_T^{VV} the coupling of the resonance to the VV component in isospin $I = 0(1, 1/2)$ and spin $S = 2$. Eq. (1) is the representation of a resonance amplitude, for instance the $f'_2(1525)$, $a_2(1320)$, and $K_2^*(1430)$ in the present case, as shown in Fig. 3 (a). The $P_{\text{initial/final}}^{(2)}$ projects the initial and final VV pair into spin two. Then the coupling of a tensor resonance to VV is given by the diagram of Fig. 3 (b), and is expressed in terms of the following vertex [16]

$$t_{R \rightarrow VV} = g_T^{VV} P_{\text{initial}}^{(2)}, \quad (4)$$

where the values for g_T^{VV} are shown in Table I. The values for $f'_2(1525)$ and $K_2^*(1430)$ are taken from Ref. [7], while those values for $a_2(1320)$ are taken from Ref. [36].

The γ - V conversion vertex can be obtained from the local hidden gauge Lagrangians [12–15] (see Ref. [37] for a practical set of rules) and one has [38]

$$-it_{\gamma V} = -iC_{\gamma V} \frac{eM_V^2}{g} \epsilon_\mu(V) \epsilon^\mu(\gamma), \quad (5)$$

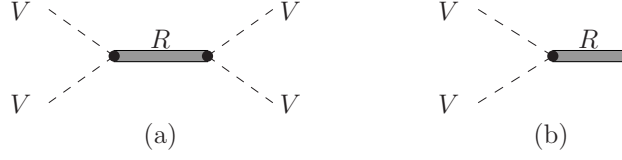


FIG. 3: (a): The $VV \rightarrow VV$ amplitude dominated by the $f'_2(1525)$, $a_2(1320)$ or $K_2^*(1430)$ pole; (b): Representation of the $f'_2(1525)$, $a_2(1320)$ or $K_2^*(1430)$ coupling to VV .

TABLE I: The coupling constants of $f'_2(1525)$, $K_2^*(1430)$, and $a_2(1320)$ to VV . The values for $f'_2(1525)$ and $K_2^*(1430)$ are taken from Ref. [7], while those for $a_2(1320)$ are taken from Ref. [36].

Resonance	Channel	g_T^{VV} (MeV)
$f'_2(1525)$	$\rho\rho$	$(-2443, i649)$
	$\omega\omega$	$(-2709, i8)$
	$\phi\omega$	$(5016, -i17)$
$K_2^*(1430)$	ρK^*	$(10901, -i71)$
	ωK^*	$(2267, -i13)$
	ϕK^*	$(-2898, i17)$
$a_2(1320)$	$\rho\omega$	$(0, -i8402)$
	$\rho\phi$	$(0, -i1912)$

with

$$g = \frac{M_\rho}{2f}; \quad f = 93 \text{ MeV}; \quad \frac{e^2}{4\pi} = \frac{1}{137}, \quad (6)$$

and

$$C_{\gamma\rho} = \frac{1}{\sqrt{2}}; \quad C_{\gamma\omega} = \frac{1}{3\sqrt{2}}; \quad C_{\gamma\phi} = -\frac{1}{3}. \quad (7)$$

The other ingredient that we need is the vector-baryon-baryon vertex, which is given by the Lagrangian

$$\mathcal{L}_{BBV} = g(< \bar{B}\gamma^\mu[V_\mu, B] > + < \bar{B}\gamma^\mu B > < V_\mu >). \quad (8)$$

From this, one can easily obtain the $\rho^0 pp$, ωpp , $K^{*+}p\Lambda$, $K^{*+}p\Sigma^0$, and $K^{*0}p\Sigma^+$ vertices,

$$-it_{\rho^0 pp} = i\frac{g}{\sqrt{2}}\bar{p}\gamma^\mu p\epsilon_\mu(\rho^0), \quad (9)$$

$$-it_{\omega pp} = i\frac{3g}{\sqrt{2}}\bar{p}\gamma^\mu p\epsilon_\mu(\omega), \quad (10)$$

$$-it_{K^{*+}p\Lambda} = -i\frac{3g}{\sqrt{6}}\bar{\Lambda}\gamma^\mu p\epsilon_\mu(K^*), \quad (11)$$

$$-it_{K^{*+}p\Sigma^0} = -i\frac{g}{\sqrt{2}}\bar{\Sigma}\gamma^\mu p\epsilon_\mu(K^*), \quad (12)$$

$$-it_{K^{*0}p\Sigma^+} = -ig\bar{\Sigma}\gamma^\mu p\epsilon_\mu(K^*). \quad (13)$$

There is one more subtlety to consider. The amplitude of Eq. (1) is evaluated for a VV state in the unitary

normalization, which for $I = 0$, $I = 1/2$ and $I = 1$ are given as follows (recall $|\rho^+ \rangle = -|1, +1 \rangle$),

$$|\rho\rho, I = 0 \rangle = -\frac{1}{\sqrt{6}}(\rho^+ \rho^- + \rho^- \rho^+ + \rho^0 \rho^0), \quad (14)$$

$$|\omega\omega, I = 0 \rangle = \frac{1}{\sqrt{2}}(\omega\omega), \quad (15)$$

$$|\phi\omega, I = 0 \rangle = (\phi\omega), \quad (16)$$

$$\begin{aligned} |\rho K^*, I = 1/2, I_3 = 1/2 \rangle &= \sqrt{\frac{2}{3}}(\rho^+ K^{*0}), \\ &-\sqrt{\frac{1}{3}}(\rho^0 K^{*+}), \end{aligned} \quad (17)$$

$$\begin{aligned} |\rho K^*, I = 1/2, I_3 = -1/2 \rangle &= \sqrt{\frac{1}{3}}(\rho^0 K^{*0}), \\ &-\sqrt{\frac{2}{3}}(\rho^- K^{*+}), \end{aligned} \quad (18)$$

$$|\omega K^*, I = 1/2 \rangle = (\omega K^*), \quad (19)$$

$$|\phi K^*, I = 1/2 \rangle = (\phi K^*), \quad (20)$$

$$|\rho\omega, I = 1 \rangle = (\rho\omega), \quad (21)$$

$$|\rho\phi, I = 1 \rangle = (\rho\phi). \quad (22)$$

Considering the vertices described above, we obtain the weights W_T^{VV} for $\gamma p \rightarrow f'_2(1525)p$, $\gamma p \rightarrow a_2^0(1320)p$ and $\gamma p \rightarrow K_2^*(1430)\Lambda(\Sigma)$ reactions (Table II). They account for the factor of Eq. (5), Eqs. (9-13), the components of the VV state in the good normalization and the couplings of the resonances to the VV channel. In the case of two identical particles the coupling is multiplied by an extra factor of $\sqrt{2}$ to restore the good normalization from the couplings calculated in Ref. [7] in the unitary approach as shown in Eqs. (14-20).

TABLE II: Weights for the $\gamma p \rightarrow f'_2(1525)p$, $\gamma p \rightarrow a_2^0(1320)p$ and $\gamma p \rightarrow K_2^*(1430)\Lambda(\Sigma)$ reactions. The $f'_2(1525)$ and $K_2^*(1430)$ are abbreviated as f'_2 and K_2^* , respectively.

Reaction		W_T^{VV}
$\gamma p \rightarrow f'_2(1525)p$	$\rho^0 \rho^0$	$-\frac{e}{\sqrt{6}}g_{f'_2}^{\rho\rho}$
	$\omega\omega$	$\frac{e}{\sqrt{2}}g_{f'_2}^{\omega\omega}$
	$\phi\omega$	$-\frac{e}{\sqrt{2}}g_{f'_2}^{\phi\omega}$
$\gamma p \rightarrow a_2^0(1320)p$	$\rho^0 \omega$	$\frac{3e}{2}g_{a_2}^{\rho\omega}$
	$\omega\rho^0$	$\frac{e}{6}g_{a_2}^{\rho\omega}$
	$\phi\rho^0$	$-\frac{e}{3\sqrt{2}}g_{a_2}^{\rho\phi}$
$\gamma p \rightarrow K_2^{*+}(1430)\Lambda$	$\rho^0 K^{*+}$	$\frac{e}{2}g_{K_2^*}^{\rho K^*}$
	ωK^{*+}	$-\frac{e}{2\sqrt{3}}g_{K_2^*}^{\omega K^*}$
	ϕK^{*+}	$\frac{e}{\sqrt{6}}g_{K_2^*}^{\phi K^*}$
$\gamma p \rightarrow K_2^{*+}(1430)\Sigma^0$	$\rho^0 K^{*+}$	$\frac{e}{2\sqrt{3}}g_{K_2^*}^{\rho K^*}$
	ωK^{*+}	$-\frac{e}{6}g_{K_2^*}^{\omega K^*}$
	ϕK^{*+}	$\frac{e}{3\sqrt{2}}g_{K_2^*}^{\phi K^*}$
$\gamma p \rightarrow K_2^{*0}(1430)\Sigma^+$	$\rho^0 K^{*0}$	$-\frac{e}{\sqrt{6}}g_{K_2^*}^{\rho K^*}$
	ωK^{*0}	$-\frac{e}{3\sqrt{2}}g_{K_2^*}^{\omega K^*}$
	ϕK^{*0}	$\frac{e}{3}g_{K_2^*}^{\phi K^*}$

Gauge invariance imposes a stringent constraint on photonuclear processes, although sometimes not all of the terms needed to have gauge invariance are numerically relevant [39, 40]. Nevertheless, in the present case, a thorough study of gauge invariance was conducted in Ref. [37] for the radiative decay of axial vector mesons within the local hidden gauge approach, and in particular in Ref. [16] for the amplitude $\rho\rho \rightarrow \rho\gamma$, which is similar to what we have here,

with the two vector mesons interacting to produce the tensor states. There it is concluded that gauge invariance is encoded in the effective coupling of the tensor states to the two vector mesons.

Considering the weights given above, the T matrix for the diagram of Fig. 1 is given by

$$\begin{aligned}
 -iT_{\gamma p \rightarrow f'_2(1525)p} &= -ie\left(-\frac{g_{f'_2}^{\rho\rho}}{\sqrt{6}} + \frac{g_{f'_2}^{\omega\omega}}{\sqrt{2}} - \frac{g_{f'_2}^{\phi\omega}}{\sqrt{2}}\right) \\
 &\left\{\frac{1}{2}[\epsilon_i(\gamma)\epsilon_j(V) + \epsilon_j(\gamma)\epsilon_i(V)] - \frac{1}{3}\epsilon_m(\gamma)\epsilon_m(V)\delta_{ij}\right\} \\
 &\frac{1}{q^2 - m_V^2} < p(M') | \gamma^\mu \epsilon_\mu(V) | p(M) >,
 \end{aligned} \tag{23}$$

$$\begin{aligned}
 -iT_{\gamma p \rightarrow a_2^0(1320)p} &= -ie\left(\frac{5g_{a_2}^{\rho\omega}}{3} - \frac{g_{a_2}^{\rho\phi}}{3\sqrt{2}}\right) \\
 &\left\{\frac{1}{2}[\epsilon_i(\gamma)\epsilon_j(V) + \epsilon_j(\gamma)\epsilon_i(V)] - \frac{1}{3}\epsilon_m(\gamma)\epsilon_m(V)\delta_{ij}\right\} \\
 &\frac{1}{q^2 - m_V^2} < p(M') | \gamma^\mu \epsilon_\mu(V) | p(M) >,
 \end{aligned} \tag{24}$$

with M and M' the third spin component of the initial and final proton. The V stands for the exchanged ρ^0 or ω . We take $m_V = m_\rho = m_\omega = 780$ MeV in the present calculation. Next, we perform the sum over the polarizations of the vector meson exchanged in Fig. 1 and then we obtain

$$\begin{aligned}
 T_{\gamma p \rightarrow f'_2(1525)p} &= e\left(-\frac{g_{f'_2}^{\rho\rho}}{\sqrt{6}} + \frac{g_{f'_2}^{\omega\omega}}{\sqrt{2}} - \frac{g_{f'_2}^{\phi\omega}}{\sqrt{2}}\right) \frac{1}{q^2 - m_V^2} \\
 &\left[\frac{1}{2}\epsilon_i(\gamma)\left(-g_{j\mu} + \frac{q_j q_\mu}{m_V^2}\right) + \frac{1}{2}\epsilon_j(\gamma)\left(-g_{i\mu} + \frac{q_i q_\mu}{m_V^2}\right) \right. \\
 &\left. - \frac{1}{3}\epsilon_m(\gamma)\delta_{ij}\left(-g_{m\mu} + \frac{q_m q_\mu}{m_V^2}\right)\right] \\
 &< p(M') | \gamma^\mu | p(M) >.
 \end{aligned} \tag{25}$$

$$\begin{aligned}
 T_{\gamma p \rightarrow a_2^0(1320)p} &= e\left(\frac{5g_{a_2}^{\rho\omega}}{3} - \frac{g_{a_2}^{\rho\phi}}{3\sqrt{2}}\right) \frac{1}{q^2 - m_V^2} \\
 &\left[\frac{1}{2}\epsilon_i(\gamma)\left(-g_{j\mu} + \frac{q_j q_\mu}{m_V^2}\right) + \frac{1}{2}\epsilon_j(\gamma)\left(-g_{i\mu} + \frac{q_i q_\mu}{m_V^2}\right) \right. \\
 &\left. - \frac{1}{3}\epsilon_m(\gamma)\delta_{ij}\left(-g_{m\mu} + \frac{q_m q_\mu}{m_V^2}\right)\right] \\
 &< p(M') | \gamma^\mu | p(M) >.
 \end{aligned} \tag{26}$$

Following the same procedure, we obtain the transition amplitudes for $\gamma p \rightarrow K_2^*(1430)\Lambda(\Sigma)$:

$$\begin{aligned}
T_{\gamma p \rightarrow K_2^{*+}(1430)\Lambda} &= e \left(\frac{g_{K_2^*}^{\rho K^*}}{2} - \frac{g_{K_2^*}^{\omega K^*}}{2\sqrt{3}} + \frac{g_{K_2^*}^{\phi K^*}}{\sqrt{6}} \right) \\
&\frac{1}{q^2 - m_{K^*}^2} \left[\frac{1}{2} \epsilon_i(\gamma) (-g_{j\mu} + \frac{q_j q_\mu}{m_{K^*}^2}) \right. \\
&+ \frac{1}{2} \epsilon_j(\gamma) (-g_{i\mu} + \frac{q_i q_\mu}{m_{K^*}^2}) - \frac{1}{3} \epsilon_m(\gamma) \delta_{ij} (-g_{m\mu} + \frac{q_m q_\mu}{m_{K^*}^2}) \left. \right] \\
&\times \langle \Lambda(M') | \gamma^\mu | p(M) \rangle, \tag{27}
\end{aligned}$$

$$\begin{aligned}
T_{\gamma p \rightarrow K_2^{*+}(1430)\Sigma^0} &= e \left(\frac{g_{K_2^*}^{\rho K^*}}{2\sqrt{3}} - \frac{g_{K_2^*}^{\omega K^*}}{6} + \frac{g_{K_2^*}^{\phi K^*}}{3\sqrt{2}} \right) \\
&\frac{1}{q^2 - m_{K^*}^2} \left[\frac{1}{2} \epsilon_i(\gamma) (-g_{j\mu} + \frac{q_j q_\mu}{m_{K^*}^2}) \right. \\
&+ \frac{1}{2} \epsilon_j(\gamma) (-g_{i\mu} + \frac{q_i q_\mu}{m_{K^*}^2}) - \frac{1}{3} \epsilon_m(\gamma) \delta_{ij} (-g_{m\mu} + \frac{q_m q_\mu}{m_{K^*}^2}) \left. \right] \\
&\times \langle \Sigma(M') | \gamma^\mu | p(M) \rangle, \tag{28}
\end{aligned}$$

$$\begin{aligned}
T_{\gamma p \rightarrow K_2^{*0}(1430)\Sigma^+} &= e \left(-\frac{g_{K_2^*}^{\rho K^*}}{\sqrt{6}} - \frac{g_{K_2^*}^{\omega K^*}}{3\sqrt{2}} + \frac{g_{K_2^*}^{\phi K^*}}{3} \right) \\
&\frac{1}{q^2 - m_{K^*}^2} \left[\frac{1}{2} \epsilon_i(\gamma) (-g_{j\mu} + \frac{q_j q_\mu}{m_{K^*}^2}) \right. \\
&+ \frac{1}{2} \epsilon_j(\gamma) (-g_{i\mu} + \frac{q_i q_\mu}{m_{K^*}^2}) - \frac{1}{3} \epsilon_m(\gamma) \delta_{ij} (-g_{m\mu} + \frac{q_m q_\mu}{m_{K^*}^2}) \left. \right] \\
&\times \langle \Sigma(M') | \gamma^\mu | p(M) \rangle, \tag{29}
\end{aligned}$$

where we take $m_{K^*} = m_{K^{*+}} = m_{K^{*0}} = 893.1$ MeV.

In Eqs. (25)-(29), the latin indices run over 1, 2, 3 and the μ index over 0, 1, 2, 3.

Then one can easily calculate $\sum \sum |T|^2$, the modulus squared of the amplitude, summing and averaging over final and initial proton spins. Here we give explicitly the case of the $\gamma p \rightarrow f_2'(1525)p$ reaction, as an example,

$$\begin{aligned}
\sum_{\gamma} \sum_{\text{pol.}} |T|^2 &= \frac{e^2}{96m_p^2(q^2 - m_V^2)^2} \left| -\frac{g_{f_2'}^{\rho\rho}}{\sqrt{6}} + \frac{g_{f_2'}^{\omega\omega}}{\sqrt{2}} - \frac{g_{f_2'}^{\phi\omega}}{\sqrt{2}} \right|^2 \\
&\sum_{i,j,m,l} \sum_{\mu,\mu'} \left[\frac{1}{2} \epsilon_i(\gamma) (-g_{j\mu} + \frac{q_j q_\mu}{m_V^2}) \right. \\
&+ \frac{1}{2} \epsilon_j(\gamma) (-g_{i\mu} + \frac{q_i q_\mu}{m_V^2}) - \frac{1}{3} \epsilon_m(\gamma) \delta_{ij} (-g_{m\mu} + \frac{q_m q_\mu}{m_V^2}) \left. \right] \\
&\left[\frac{1}{2} \epsilon_i(\gamma) (-g_{j\mu'} + \frac{q_j q_{\mu'}}{m_V^2}) + \frac{1}{2} \epsilon_j(\gamma) (-g_{i\mu'} + \frac{q_i q_{\mu'}}{m_V^2}) \right. \\
&- \frac{1}{3} \epsilon_l(\gamma) \delta_{ij} (-g_{l\mu'} + \frac{q_l q_{\mu'}}{m_V^2}) \left. \right] \\
&Tr[(\not{p}' + m_p) \gamma^\mu (\not{p} + m_p) \gamma^{\mu'}], \tag{30}
\end{aligned}$$

where all the indices and the two photon polarizations should be summed over, with the following expressions of the latter,

$$\epsilon^{(1)}(\gamma) = \begin{pmatrix} 1 \\ 0 \\ 0 \end{pmatrix}; \quad \epsilon^{(2)}(\gamma) = \begin{pmatrix} 0 \\ 1 \\ 0 \end{pmatrix}, \tag{31}$$

where we have assumed that the photon travels in the Z direction.

The hypothesis that the tensor resonances considered are dynamically generated leads to the mechanism depicted in Figs. 1 and 2, where one vector meson appears in the t -channel. This is then a process which is t -channel dominated.

As such, it leads to a particular t -dependence in the cross section, which can be tested experimentally. In the work of Ref. [23], where the photoproduction of the $f_2(1270)$ was studied along the same lines as here, it was found that the t -dependence of the model was in fair agreement with the experiment [24]. Processes led by t -channel meson exchange are quite common in hadron physics. Even the chiral Lagrangians, which are given by contact terms, can be reinterpreted in terms of t -channel vector meson exchange within the framework of the local hidden gauge approach [12–15]. However, terms involving u -channel exchange or s -channel propagation are also possible, but lead to different t -dependence that experiment can in principle disentangle. Yet, in the present case, the assumption of the large coupling of the resonances to vector-vector leads us to this t -channel exchange mechanism.

It is also interesting to argue in a different direction. Let us assume that the process is t -channel dominated. Then it is worth noting that due to C -parity conservation it must be a vector meson that is exchanged, scalars and pseudoscalar exchange are excluded. This only holds if the exchanged particle is a neutral one, which can have a given C -parity, but not if the exchanged particle is charged. This latter case is the one that one finds in the $\gamma p \rightarrow na_2^+(1320)$ reaction which was studied in Ref. [41] and Ref. [42] by means of a charged pion exchange. The fact that we have the $\gamma p \rightarrow pR$ precludes the contribution of those mechanisms and is selective only to the coupling of the resonance R to the vector-vector components. This is why we also consider the a_2 resonance, since, even if other components could be relevant in its wave function, this process would be selective of the vector-vector component.

B. Differential cross section

The differential cross section for $\gamma p \rightarrow f_2'(1525)p$, $\gamma p \rightarrow K_2^*(1430)\Lambda(\Sigma)$, and $\gamma p \rightarrow a_2^0(1320)p$ reactions are given by

$$\frac{d\sigma}{dt} = \frac{m_i^2}{16\pi s|\vec{k}|^2} \sum \sum |T|^2, \quad (32)$$

where we are summing and averaging over final and initial proton spins, with s the invariant mass squared of the γp system, and $m_i^2 = m_p^2$ for $\gamma p \rightarrow f_2'(1525)p$ and $\gamma p \rightarrow a_2^0(1320)p$ reactions, $m_i^2 = m_p m_\Lambda$ for $\gamma p \rightarrow K_2^{*+}(1430)\Lambda$ reaction, and $m_i^2 = m_p m_\Sigma$ for $\gamma p \rightarrow K_2^*(1430)\Sigma$ reaction.² The variable \vec{k} is the three momentum of the initial photon in the center of mass frame (c.m.), and $t = q^2 = (p - p')^2$.

The Eq. (32) can be generalized for the case when the $f_2'(1525)$ ($K_2^*(1430)$, or $a_2(1320)$) is explicitly allowed to decay into $K\bar{K}$ ($K\pi$ or $\eta\pi$) by working out the three body phase space and we find

$$\begin{aligned} \frac{d^2\sigma}{dM_{\text{inv}}dt} &= \frac{m_i^2}{8\pi^2 s|\vec{k}|^2} \frac{M_{\text{inv}}^2 \Gamma_i}{|M_{\text{inv}}^2 - M_R^2 + iM_{\text{inv}}\Gamma_R|^2} \\ &\times \sum \sum |T|^2, \end{aligned} \quad (33)$$

where M_{inv} is the invariant mass distribution of the $K\bar{K}$ or $K\pi$, Γ_R is the total decay width of the $f_2'(1525)$, $K_2^*(1430)$ or $a_2(1320)$ and Γ_i is the partial decay width of the $f_2'(1525) \rightarrow K\bar{K}$, $K_2^*(1430) \rightarrow K\pi$ or $a_2(1320) \rightarrow \eta\pi$. In the present study, we choose the following decay modes: $f_2'(1525) \rightarrow K^+K^-$, $K_2^{*+}(1430) \rightarrow K^0\pi^+$, $K_2^{*0}(1430) \rightarrow K^+\pi^-$, and $a_2^0(1320) \rightarrow \eta\pi^0$. The $f_2'(1525) \rightarrow K^+K^-$ decay accounts for 1/2 of the $K\bar{K}$ decay of the $f_2'(1525)$ which is 89% of the $\Gamma_{f_2'(1525)}$, while the $K_2^{*+}(1430) \rightarrow K^0\pi^+$ or $K_2^{*0}(1430) \rightarrow K^+\pi^-$ decay accounts for 2/3 of the $K\pi$ decay of the $K_2^*(1430)$ which is 50% of $\Gamma_{K_2^*(1430)}$. The $a_2^0(1320) \rightarrow \eta\pi^0$ is 14.5% of the $\Gamma_{a_2(1320)}$. Since the $f_2'(1525) \rightarrow K\bar{K}$, $K_2^*(1430) \rightarrow K\pi$, and $a_2(1320) \rightarrow \eta\pi$ decays are in D -wave, in order to have Γ_i and Γ_R in the range of invariant masses that we consider, we take

$$\Gamma_{f_2' \rightarrow K\bar{K}}(M_{\text{inv}}) = \Gamma_{K\bar{K}}^{\text{on}} \left(\frac{\tilde{q}_{K\bar{K}}}{\bar{q}_{K\bar{K}}} \right)^5 \frac{M_{f_2'}^2}{M_{\text{inv}}^2}, \quad (34)$$

$$\Gamma_{f_2'}(M_{\text{inv}}) = 0.89\Gamma_{f_2'}^{\text{on}} \left(\frac{\tilde{q}_{K\bar{K}}}{\bar{q}_{K\bar{K}}} \right)^5 \frac{M_{f_2'}^2}{M_{\text{inv}}^2} + 0.11\Gamma_{f_2'}^{\text{on}}, \quad (35)$$

² We take $m_{\Sigma^0} = m_{\Sigma^+} = 1191$ MeV and $m_{K_2^{*+}} = m_{K_2^{*0}} = 1429$ MeV in this work.

with $\Gamma_{f'_2}^{\text{on}} = 73$ MeV, $\Gamma_{K\bar{K}}^{\text{on}} = 32.5$ MeV, $M_{f'_2} = 1525$ MeV [43], and

$$\tilde{q}_{K\bar{K}} = \frac{\lambda^{1/2}(M_{\text{inv}}^2, m_K^2, m_{\bar{K}}^2)}{2M_{\text{inv}}}, \quad (36)$$

$$\bar{q}_{K\bar{K}} = \frac{\lambda^{1/2}(M_{f'_2}^2, m_K^2, m_{\bar{K}}^2)}{2M_{f'_2}}, \quad (37)$$

where λ is the Källén function with $\lambda(x, y, z) = (x - y - z)^2 - 4yz$.

Similarly, for the $K_2^*(1430)$ decay modes, we take

$$\Gamma_{K_2^* \rightarrow K\pi}(M_{\text{inv}}) = \Gamma_{K\pi}^{\text{on}} \left(\frac{\tilde{q}_{K\pi}}{\bar{q}_{K\pi}} \right)^5 \frac{M_{K_2^*}^2}{M_{\text{inv}}^2}, \quad (38)$$

$$\Gamma_{K_2^*}(M_{\text{inv}}) = 0.5\Gamma_{K_2^*}^{\text{on}} \left(\frac{\tilde{q}_{K\pi}}{\bar{q}_{K\pi}} \right)^5 \frac{M_{K_2^*}^2}{M_{\text{inv}}^2} + 0.5\Gamma_{K_2^*}^{\text{on}}, \quad (39)$$

with $\Gamma_{K_2^*}^{\text{on}} = 104$ MeV, $\Gamma_{K\pi}^{\text{on}} = 34.7$ MeV [43], and

$$\tilde{q}_{K\pi} = \frac{\lambda^{1/2}(M_{\text{inv}}^2, m_K^2, m_{\pi}^2)}{2M_{\text{inv}}}, \quad (40)$$

$$\bar{q}_{K\pi} = \frac{\lambda^{1/2}(M_{K_2^*}^2, m_K^2, m_{\pi}^2)}{2M_{K_2^*}}. \quad (41)$$

Finally, for the $a_2(1320)$ decays, we take

$$\Gamma_{a_2 \rightarrow \eta\pi}(M_{\text{inv}}) = \Gamma_{\eta\pi}^{\text{on}} \left(\frac{\tilde{q}_{\eta\pi}}{\bar{q}_{\eta\pi}} \right)^5 \frac{M_{a_2}^2}{M_{\text{inv}}^2}, \quad (42)$$

$$\Gamma_{a_2}(M_{\text{inv}}) = 0.145\Gamma_{a_2}^{\text{on}} \left(\frac{\tilde{q}_{\eta\pi}}{\bar{q}_{\eta\pi}} \right)^5 \frac{M_{a_2}^2}{M_{\text{inv}}^2} + 0.855\Gamma_{a_2}^{\text{on}}, \quad (43)$$

with $\Gamma_{a_2}^{\text{on}} = 107$ MeV, $\Gamma_{\eta\pi}^{\text{on}} = 15.5$ MeV [43], and

$$\tilde{q}_{\eta\pi} = \frac{\lambda^{1/2}(M_{\text{inv}}^2, m_{\eta}^2, m_{\pi}^2)}{2M_{\text{inv}}}, \quad (44)$$

$$\bar{q}_{\eta\pi} = \frac{\lambda^{1/2}(M_{a_2}^2, m_{\eta}^2, m_{\pi}^2)}{2M_{a_2}}. \quad (45)$$

III. NUMERICAL RESULTS

In Ref. [23] three models were considered, one is the one we exposed here, and the other two contained an additional tensor ρNN coupling and Regge propagators. The results obtained there were very similar and in this exploratory work we perform calculations only with one of the models as specified above.

In Fig. 4 we show $\frac{d^2\sigma}{dM_{\text{inv}}dt}$ for the $\gamma p \rightarrow pK^+K^-$ reaction at $E_\gamma = 3.4$ GeV and $t = -1.2$ GeV², where M_{inv} is the invariant mass of the K^+K^- system. The $f'_2(1525)$ resonance is clearly seen, peaking around $M_{\text{inv}} = 1525$ MeV with an apparent width of about 60 MeV.

In Fig. 5 we show $\frac{d^2\sigma}{dM_{\text{inv}}dt}$ for the $\gamma p \rightarrow p\eta\pi^0$ reaction at $E_\gamma = 3.4$ GeV and $t = -1.2$ GeV², where M_{inv} is the invariant mass of $\eta\pi^0$ system. The $a_2(1320)$ resonance is clearly seen, peaking around $M_{\text{inv}} = 1320$ MeV. **As we have mentioned, we expect larger uncertainties in this case. An estimate of these uncertainties can be obtained by comparing the predictions of the molecular picture for the partial decay width of the $a_2(1230) \rightarrow \pi^+\gamma$ reaction obtained in [9], $\Gamma(a_2(1230) \rightarrow \pi^+\gamma) = (196 \pm 30)$ KeV with experiment $\Gamma(a_2(1230) \rightarrow \pi^+\gamma) = (281 \pm 34)$ KeV. This comparison shows that uncertainties of the order of 50% seem realistic.**

In Fig. 6 we show $\frac{d^2\sigma}{dM_{\text{inv}}dt}$ for the $\gamma p \rightarrow \Lambda(\Sigma)K\pi$ reaction at $E_\gamma = 3.4$ GeV and $t = -1.2$ GeV², where M_{inv} is the invariant mass of the $K\pi$ system. The $K_2^*(1430)$ is clearly seen in all the three decay modes, but the magnitude of

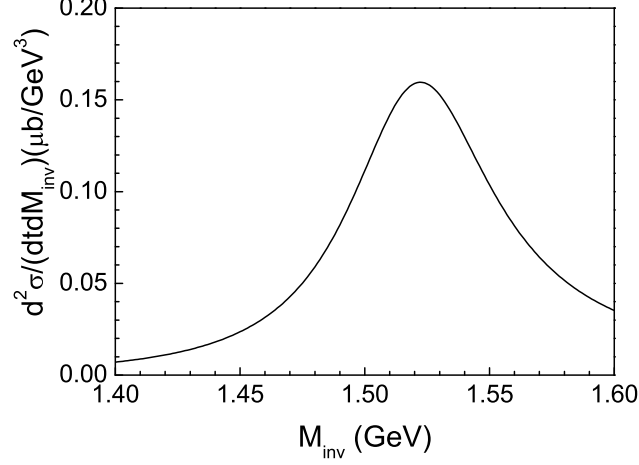


FIG. 4: Theoretical predictions for the D -wave $K\bar{K}$ mass distribution of the $\gamma p \rightarrow pK^+K^-$ reaction at $E_\gamma = 3.4$ GeV and $t = -1.2$ GeV².

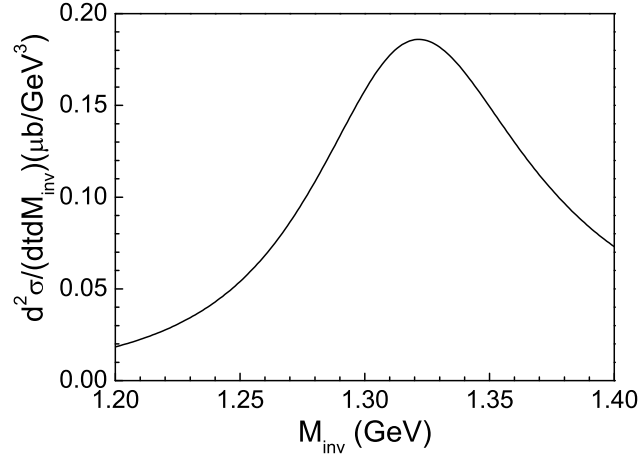


FIG. 5: Theoretical predictions for the D -wave $\eta\pi^0$ mass distribution of the $\gamma p \rightarrow p\eta\pi^0$ reaction at $E_\gamma = 3.4$ GeV and $t = -1.2$ GeV².

the decay modes are quite different. Experimental confirmation of such a hierarchy constitutes a valid check of the molecular picture of the $K_2^*(1430)$ and the reaction mechanism advocated here.

Fig. 7 shows $d\sigma/dt$ at $E_\gamma = 3.4$ GeV for the five reaction modes studied. We see that the slopes for the five reactions are quite similar.

In addition to the differential cross section, we calculate also the total cross section for the five reactions as a function of the photon beam energy E_γ . The results are shown in Fig. 8. The cross sections increase rapidly away from threshold and soon become almost constant at higher photon energies.

We stress again that the reaction formalism advocated here involves no free parameters, which allow us to make predictions for total cross sections. The differential and total cross sections can be checked in future experiments, such as those at CLAS. In this sense, the reaction mechanism can be easily tested.

So far we can quote some preliminary results comparing $f_2(1270)$ and $f_2'(1525)$ in Ref. [44]. The $f_2(1270)$ production rate for $1.7 \text{ GeV} < E_\gamma < 5.5 \text{ GeV}$ decaying into K^+K^- is larger than that of $f_2'(1525)$, which taking into account the different $K\bar{K}$ branching ratios indicates a rate of $f_2(1270)$ production fairly bigger than that of $f_2'(1525)$. The ratio of these production rates depends on E_γ but seems to be at an order of 10, comparing the results of Ref. [23]

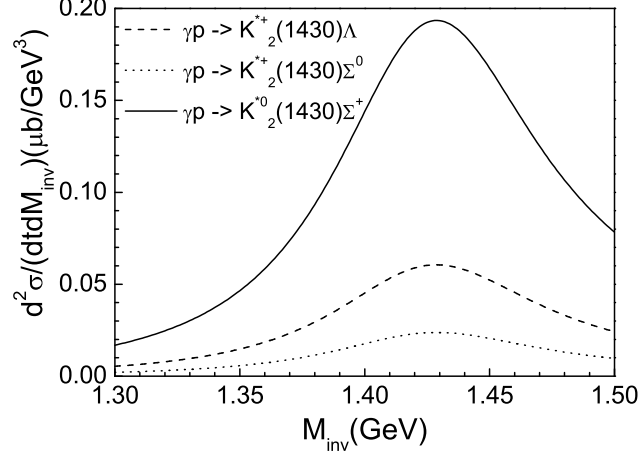


FIG. 6: Theoretical predictions for the D -wave $K\pi$ mass distribution of the $\gamma p \rightarrow \Lambda(\Sigma)K\pi$ reaction at $E_\gamma = 3.4$ GeV and $t = -1.2$ GeV²

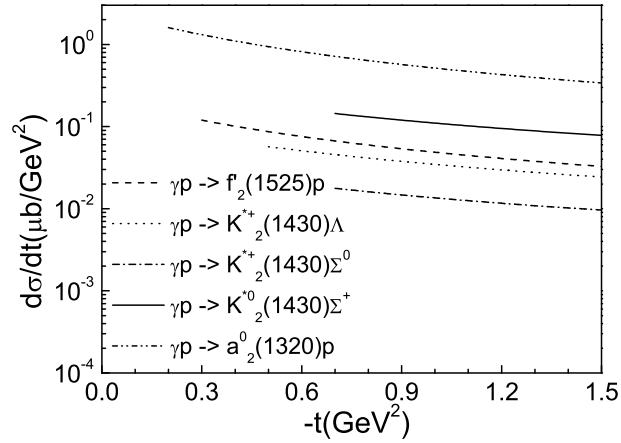


FIG. 7: Differential cross sections $\frac{d\sigma}{dt}$ as functions of t at $E_\gamma = 3.4$ GeV.

and those here, .

IV. CONCLUSIONS

In recent years, it has been found that the $f'_2(1525)$, $a_2(1320)$, and $K_2^*(1430)$ resonances, though long been accepted as ordinary $q\bar{q}$ states, can be dynamically generated from the vector meson-vector meson interaction, and therefore qualify as vector-vector molecules. Many tests adopting such a scenario have been performed in mesonic reactions and all yield positive results. In the present work, we have proposed to test the molecular picture in the photonuclear reaction. The elements needed for the test are very simple, which makes the interpretation of the results particularly transparent. On one side the $f'_2(1525)$, $a_2(1320)$ and $K_2^*(1430)$ couple to VV in $I = 0$, $I = 1$ and $I = 1/2$, respectively, and the couplings have been fixed before in the unitary approach that generates the $f'_2(1525)$, $a_2(1320)$, $K_2^*(1430)$ as VV molecules based on the local hidden gauge formalism for the interaction of vector mesons. On the other side, with these couplings and the vector meson dominance hypothesis, incorporated in the local hidden gauge approach, the photon gets converted into one of the vector mesons, which interact with the vector meson emitted by the incoming

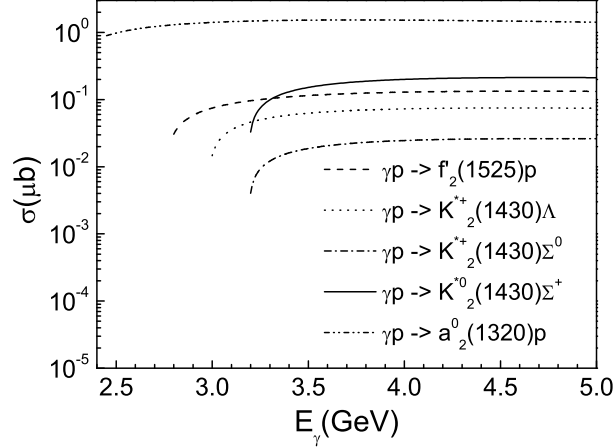


FIG. 8: Total cross sections for the $\gamma p \rightarrow f'_2(1525)p$, $\gamma p \rightarrow a^0_2(1320)p$ and $\gamma p \rightarrow K^*_2(1430)\Lambda(\Sigma)$ reactions as functions of E_γ .

proton to generate the $f'_2(1525)$, $a_2(1320)$ and $K^*_2(1430)$ resonances. With this simple picture we predict both the differential and total cross sections, which could be tested by future experiments, such as those at CLAS. **The case of the $a_2(1320)$ might have more uncertainties which we have quantified by looking at the predictions for the $a_2(1320) \rightarrow \pi^+\gamma$ reaction comparing them with experiment.**

Acknowledgments

One of us, E. O., wishes to acknowledge support from the Chinese Academy of Science (CAS) in the Program of Visiting Professorship for Senior International Scientists (Grant No. 2013T2J0012). L.S.G. thanks the Institute for Nuclear Theory at University of Washington for its hospitality and the Department of Energy for partial support during the completion of this work. This work is partly supported by the Spanish Ministerio de Economía y Competitividad and European FEDER funds under the contract number FIS2011-28853-C02-01 and FIS2011-28853-C02-02, and the Generalitat Valenciana in the program Prometeo II-2014/068. We acknowledge the support of the European Community-Research Infrastructure Integrating Activity Study of Strongly Interacting Matter (acronym HadronPhysics3, Grant Agreement n. 283286) under the Seventh Framework Programme of EU. This work is also partly supported by the National Natural Science Foundation of China under Grant Nos. 11475227, 1375024, and 11522539. This work is also supported by the Open Project Program of State Key Laboratory of Theoretical Physics, Institute of Theoretical Physics, Chinese Academy of Sciences, China (No.Y5KF151CJ1).

-
- [1] R. Aaij *et al.* [LHCb Collaboration], Phys. Rev. Lett. **115**, 072001 (2015).
 - [2] S. L. Olsen, Front. Phys. China. **10**, 121 (2015).
 - [3] X. Liu, Chin. Sci. Bull. **59**, 3815 (2014).
 - [4] G. T. Bodwin, E. Braaten, E. Eichten, S. L. Olsen, T. K. Pedlar and J. Russ, arXiv:1307.7425.
 - [5] N. Brambilla *et al.*, Eur. Phys. J. C **71**, 1534 (2011).
 - [6] R. Molina, D. Nicmorus and E. Oset, Phys. Rev. D **78**, 114018 (2008).
 - [7] L. S. Geng and E. Oset, Phys. Rev. D **79**, 074009 (2009).
 - [8] L. S. Geng, E. Oset, R. Molina and D. Nicmorus, PoS EFT **09**, 040 (2009).
 - [9] R. Molina, H. Nagahiro, A. Hosaka and E. Oset, Phys. Rev. D **83**, 094030 (2011).
 - [10] A. K. Rai and D. P. Rathaud, Eur. Phys. J. C **75**, 462 (2015).
 - [11] W. L. Wang and Z. Y. Zhang, Phys. Rev. C **84**, 054006 (2011).
 - [12] M. Bando, T. Kugo, S. Uehara, K. Yamawaki and T. Yanagida, Phys. Rev. Lett. **54**, 1215 (1985).
 - [13] M. Bando, T. Kugo and K. Yamawaki, Phys. Rept. **164**, 217 (1988).
 - [14] M. Harada and K. Yamawaki, Phys. Rept. **381**, 1 (2003).
 - [15] U. G. Meissner, Phys. Rept. **161**, 213 (1988).

- [16] H. Nagahiro, J. Yamagata-Sekihara, E. Oset, S. Hirenzaki and R. Molina, Phys. Rev. D **79**, 114023 (2009).
- [17] T. Branz, L. S. Geng and E. Oset, Phys. Rev. D **81**, 054037 (2010).
- [18] A. Martinez Torres, L. S. Geng, L. R. Dai, B. X. Sun, E. Oset and B. S. Zou, Phys. Lett. B **680**, 310 (2009).
- [19] L. S. Geng, F. K. Guo, C. Hanhart, R. Molina, E. Oset and B. S. Zou, Eur. Phys. J. A **44**, 305 (2010).
- [20] L. Dai and E. Oset, Eur. Phys. J. A **49**, 130 (2013).
- [21] L. R. Dai, J. J. Xie and E. Oset, Phys. Rev. D **91**, 094013 (2015).
- [22] J. J. Xie and E. Oset, Phys. Rev. D **90**, 094006 (2014).
- [23] J. J. Xie and E. Oset, Eur. Phys. J. A **51**, 111 (2015).
- [24] M. Battaglieri *et al.* [CLAS Collaboration], Phys. Rev. D **80**, 072005 (2009).
- [25] E. Klempt and A. Zaitsev, Phys. Rept. **454**, 1 (2007).
- [26] V. Crede and C. A. Meyer, Prog. Part. Nucl. Phys. **63**, 74 (2009).
- [27] F. Giacosa, T. Gutsche, V. E. Lyubovitskij and A. Faessler, Phys. Rev. D **72**, 114021 (2005).
- [28] V. Cirigliano, G. Ecker, H. Neufeld and A. Pich, JHEP **0306**, 012 (2003).
- [29] G. Ecker, J. Gasser, A. Pich and E. de Rafael, Nucl. Phys. B **321**, 311 (1989).
- [30] G. Ecker, J. Gasser, H. Leutwyler, A. Pich and E. de Rafael, Phys. Lett. B **223**, 425 (1989).
- [31] L. S. Geng, E. Oset, R. Molina, A. Martinez Torres, T. Branz, F. K. Guo, L. R. Dai and B. X. Sun, AIP Conf. Proc. **1322**, 214 (2010).
- [32] D. Jido, J. A. Oller, E. Oset, A. Ramos and U. G. Meissner, Nucl. Phys. A **725**, 181 (2003).
- [33] C. Garcia-Recio, M. F. M. Lutz and J. Nieves, Phys. Lett. B **582**, 49 (2004).
- [34] M. F. M. Lutz and I. Vidana, Eur. Phys. J. A **48**, 124 (2012).
- [35] M. F. M. Lutz, E. E. Kolomeitsev and C. L. Korpa, Phys. Rev. D **92**, 016003 (2015).
- [36] C. Garca-Recio, L. S. Geng, J. Nieves, L. L. Salcedo, E. Wang and J. J. Xie, Phys. Rev. D **87**, 096006 (2013).
- [37] H. Nagahiro, L. Roca, A. Hosaka and E. Oset, Phys. Rev. D **79**, 014015 (2009).
- [38] A. Ramos and E. Oset, Phys. Lett. B **727**, 287 (2013).
- [39] B. Borasoy, P. C. Bruns, U.-G. Meissner and R. Nissler, Phys. Rev. C **72**, 065201 (2005).
- [40] M. Doring, E. Oset and D. Strottman, Phys. Rev. C **73**, 045209 (2006).
- [41] X. Y. Wang and A. Guskov, arXiv:1510.00898 [hep-ph].
- [42] Y. Huang, J. J. Xie, X. R. Chen, J. He and H. F. Zhang, Int. J. Mod. Phys. E **23**, 1460002 (2014).
- [43] K. A. Olive *et al.* [Particle Data Group Collaboration], Chin. Phys. C **38**, 090001 (2014).
- [44] Rafael A. Badui, Jason Bono, Lei Guo, and Brian Raue, talk at the Hadron Conference 2015, https://www.jlab.org/conferences/hadron2015/talks/friday/parallel/session2/2D4_RafaelBadui.pdf.